

pubs.acs.org/Macromolecules Article

Unified Entanglement Scaling for Flexible, Semiflexible, and Stiff Polymer Melts and Solutions

Scott T. Milner*



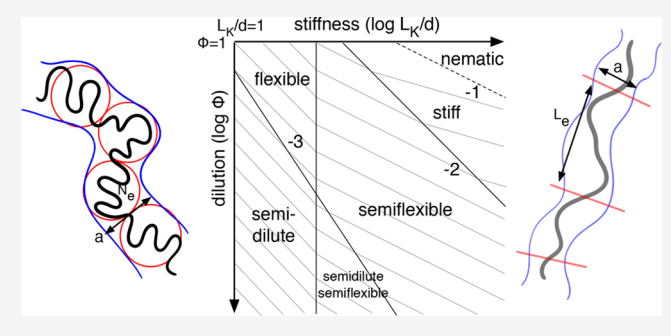
Cite This: Macromolecules 2020, 53, 1314-1325



ACCESS

Metrics & More

ABSTRACT: The entanglement length $N_{\rm e}$ is a key parameter for all entangled polymer fluids for which no comprehensive scaling theory yet exists. We have pieces of a theory; the Lin-Noolandi (LN) argument predicts $N_{\rm e}$ scaling for flexible chains that agrees with data on polymer melts. There are arguments for how $N_{\rm e}$ should depend on polymer concentration, but which are not obviously consistent with LN. Morse scaling describes entanglement for solutions of stiff chains, consistent with data. Everaers proposed an ansatz that $N_{\rm e}$ depends only on the arclength concentration, as if chains were uncrossable threads of vanishing thickness. This ansatz is consistent with simulations of bead-spring



Article Recommendations

chains, but not with LN, as it has no role for packing length, the central parameter in LN scaling. We propose a comprehensive scaling theory that includes LN in one limit, thread ansatz in another, and reduces to Morse scaling for stiff chains. One new ingredient is that the typical distance of closest approach between two chains is governed by the packing length or chain diameter, whichever is larger. If a chain is sufficiently flexible and bulky, the packing length is relevant; but for stiffened bead-spring chains without side groups, the packing length is smaller than the chain diameter, so thread scaling applies. Our approach presents a consistent physical picture of entanglements in all regimes as close encounters between two chains. For solutions, we determine the entanglement probability between chain segments, and consistently describe the crossover between the Edwards and semidilute regimes.

■ INTRODUCTION

The entanglement length $N_{\rm e}$ and entanglement strand relaxation time $\tau_{\rm e}$ are the two key material parameters in the modern theory of flow in entangled melts and solutions. This theory, built on the tube concept as an approximate representation of uncrossability constraints, has been quantitatively successful in describing linear and nonlinear flow behavior of entangled melts and solutions of linear and branched polymers. $^{2-7}$

In tube-based theory, the many-chain problem of a melt or solution of chains that cannot cross through each other is replaced by an approximation, in the spirit of mean field theory, of a single chain confined by neighboring chains in a tube (Figure 1), which deforms with flow and relaxes as other chains explore new conformations. The single confined chain undergoes random thermal motions, which, for linear chains, cause fluctuations in the contour length, and diffusive motion back and forth along the tube called reptation. By these motions, the chain progressively explores new conformations, and stress held in the entangled network after a step strain thus decays away.

The tube diameter a expresses the range of transverse motions a chain can undergo at times short compared to the time governing its escape from the tube, which for entangled melts or solutions of linear chains is the reptation time. The entanglement length $N_{\rm e}$ (or equivalently the mass $M_{\rm e}$) is the

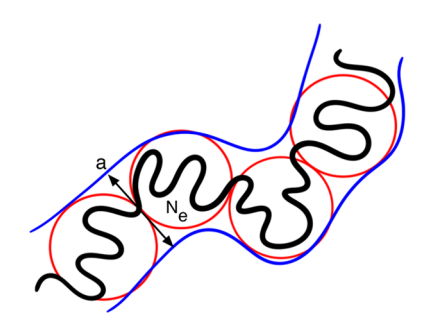


Figure 1. Cartoon of a single flexible chain confined to its tube.

length of a chain segment such that its transverse displacements from the tube centerline are of order a. The chain in its tube may be regarded as a sequence of entanglement strands of length $N_{\rm e}$, each one just long enough to "feel" the tube confinement.

Received: December 18, 2019 Published: February 5, 2020



An entangled melt or solution responds like an elastic material when it is sheared quickly. On timescales such that chains can relax their contour lengths but not yet reptate (so between the Rouse time $\tau_{\rm R}$ and reptation time $\tau_{\rm d}$), the melt or solution behaves like a rubber with a modulus $G^{\rm S,9}$ (G is called the plateau modulus because it describes the plateau in frequency-dependent response between $1/\tau_{\rm R}$ and $1/\tau_{\rm d}$.) Physically, the elastic response derives from the reduction in entropy of chain segments confined in the tube, which deforms approximately affinely as the material is sheared. Hence, rubber elasticity predicts the modulus G as kT per entanglement strand.

The tube diameter a and entanglement strand length $N_{\rm e}$ are material constants, dependent on polymer type and concentration. We would like to predict a and $N_{\rm e}$ from geometrical properties of the polymer chains alone, rather than dynamical measurements or simulations. Because there are many plausible microscopic lengths in the problem, we cannot simply infer a from dimensional analysis. Instead, we require at least a physically motivated scaling theory, which we hope will shed light on the nature of entanglements.

 $N_{\rm e}$ and a are related by the requirement that a segment of length $N_{\rm e}$ has transverse fluctuations from the tube centerline of order a. This relation involves the chain stiffness, as expressed by the Kuhn length $L_{\rm K}$. Roughly speaking, $L_{\rm K}$ is such that a chain segment of $L_{\rm K}$ "forgets" its direction from one end to the other. Stiff chains have longer Kuhn lengths, and have random-walk conformations that are more expanded. Indeed, the Kuhn length can be obtained from dimensions of sufficiently long chains as the ratio R^2/L , where R^2 is the mean-square end-to-end distance and L is the fully extended length.

The tube diameter quantifies the consequences of uncrossability and chain packing on the thermally accessible transverse motions of chain segments. In melts, the density is essentially fixed by the hard core volume of chain monomers, and chain conformations are essentially ideal Gaussian random walks, with dimensions governed by the Kuhn length. (This is because any tendency for single-chain conformations to be self-avoiding is effectively screened by the concentrated presence of other chains. Figuratively speaking, a chain exploring random-walk configurations gains nothing by avoiding itself, since it constantly undergoes collisions with other chains.)¹⁰

Therefore, we may expect that a and $N_{\rm e}$ for melts should only depend on the Kuhn length and the effective chain diameter d, defined such that the volume per chain in the melt is $\pi(d/2)^2L$. For solutions, a and $N_{\rm e}$ depend in addition on the polymer volume fraction ϕ , and may depend as well on solvent quality, which determines whether individual chains are self-avoiding, and thereby affects local chain packing.

However, except at low concentrations with good solvents, chains are not all that self-avoiding. Indeed, we define the "swelling length" $N_{\rm s}$ as the length of a chain segment in a given solvent such that its self-interactions as a Gaussian coil are of order kT. If solutions are concentrated enough that strands of length $N_{\rm s}$ typically encounter other chains, self-avoidance is suppressed by screening, just as in the melt. This sets an upper limit on ϕ for a given solvent, above which chains are ideal random walks. Therefore, in most practical circumstances, ignoring self-avoidance effects on entanglement is likely a good approximation.

Because we expect entanglement properties to depend only on chain conformations and packing (and as argued above only on L_K , d, and ϕ), simulations of coarse-grained models like beadspring chains should suffice to explore entanglement behavior,

without explicit representation of specific interactions or microscopic details of monomer shape. Likewise, scaling theories that focus on $L_{\rm K}$, d, and ϕ should suffice to make useful predictions of a and $N_{\rm e}$ for real polymers.

Indeed, there exist three different scaling theories that describe polymer entanglement in various regimes: one for flexible chains, one for stiff chains, and one ansatz that asserts entanglement properties depend on concentration ϕ only through the arclength density of chains, described below. These theories are incomplete (and in some ways mutually inconsistent), in that no single approach consistently describes melts and solutions of flexible and stiff chains. We now summarize the underlying physical assumptions of these three existing approaches, and their successes and limitations in accounting for experimental and simulation results.

The first approach, introduced by Lin and Noolandi, applies to melts of flexible polymers. $^{13-15}$ It asserts that the volume pervaded by an entanglement strand contains a fixed number of other such strands, independent of the diameter or Kuhn length of the polymer. In other words, when enough other strands cohabit the same volume as a given strand, that strand will be entangled. This leads to the prediction that the modulus G is proportional to kT/p^3 , where p is the packing length. (We will recapitulate this result in more detail in the following section.)

The packing length p is defined as the ratio V/R^2 of the chain displaced volume V and mean-square end-to-end distance R^2 . Because both scale linearly with chain mass, the ratio is a material constant with dimensions of length. It can be shown that p is the typical distance over which monomers of a given chain dominate the density. The packing length is short for stiff skinny chains, and long for flexible chains with bulky sidegroups. We can think of p as the typical distance of closest approach for two polymer strands. For a semiflexible chain with Kuhn length L_K and diameter d, p scales as d^2/L_K .

Importantly, p only depends on chain dimensions, so the LN result in that the modulus G scales as kT/p^3 predicts a dynamical consequence of entanglement from chain dimensions alone. From G, we can infer $N_{\rm e}$ (since G is kT per entanglement strand), and from chain dimensions we can infer a. This scaling theory is consistent with the measured plateau modulus and chain dimensions for a wide range of polymers (Figure 2). 16,17

It is not immediately clear how to generalize the LN scaling ansatz to solutions. The naive generalization is that each polymer strand carries with it a certain quantity of solvent, such that the polymer volume fraction in the cohabited volume

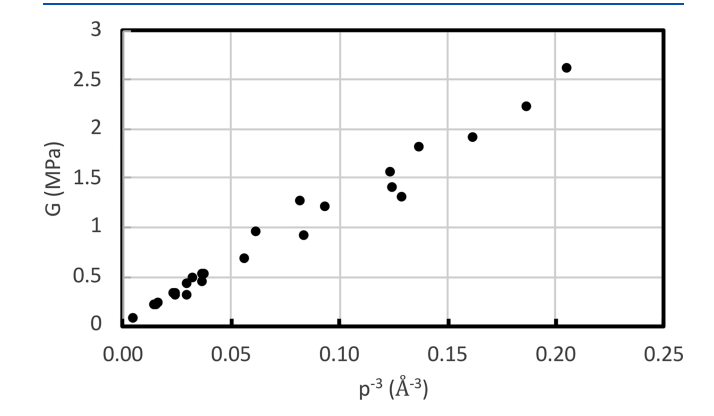


Figure 2. Plateau modulus G vs p^{-3} where p is the packing length. Adapted from Fetters et al., refs 16 and 17.

described by LN is ϕ . This leads to the incorrect prediction that G is proportional to ϕ^3 . This prediction is definitely ruled out by careful experiments on polymer solutions, which are consistent with G scaling as ϕ^2 (Figure 3). ^{18,19}

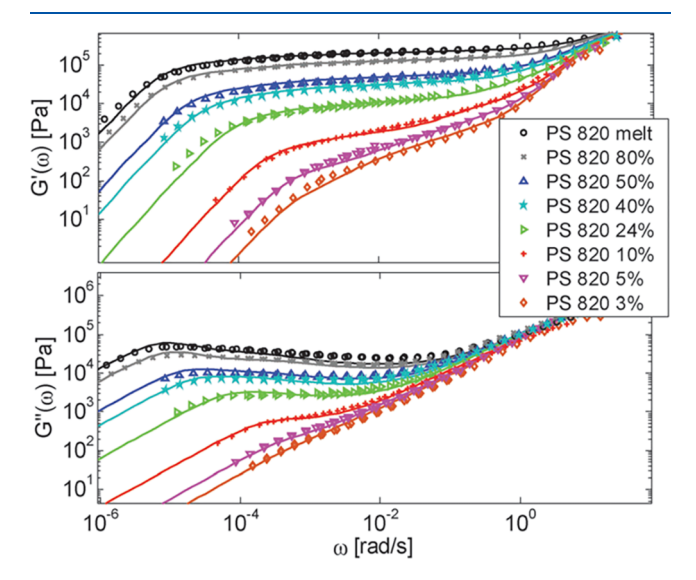


Figure 3. Fit of tube-based TMA (time-marching algorithm) model to dynamic rheology for entangled polystyrene solutions, assuming $G(\phi)$ scales as ϕ^2 (from van Ruymbeke et al., ref 19).

On reflection, this naive generalization amounts to the assumption that every chain is effectively "coated" with solvent, like insulation on a wire. This is an unrealistic assumption, because chains in solutions where self-avoidance is minimal adopt ideal random-walk configurations, and hence are uncorrelated with the solvent concentration. Rather, we may expect in solution that entanglements occur where the local chain concentration happens to be high.

If we instead assert that entanglements somehow arise from binary contacts, we can argue for a different concentration dependence of $N_{\rm e}$ (and hence G) by a dilution argument. Note that the idea of entanglements as arising from binary contacts is not obviously consistent with the LN idea of entanglement strands as defined by cohabiting the same volume. In this paper, we shall reformulate LN scaling to make this consistency clear.)

Starting with a melt, some fraction $1-\phi$ of the chains is "deleted" without changing the conformations of the remaining chains, to give a typical solution configuration. By this deletion, only a fraction ϕ of binary contacts survive along a given surviving chain. Hence $N_{\rm e}(\phi)$, the chain length between entanglements arising somehow from binary contacts, scales as $1/\phi$. The solution modulus still scales as kT per entanglement strand; because only a fraction ϕ of strands survive to contribute to the modulus, G then scales as ϕ^2 , consistent with experiment.

The LN argument assumes that chains are Gaussian random walks within their tubes, which requires that the Kuhn length is less than the tube diameter. If we stiffen chains, the Kuhn length increases, the packing length decreases, the modulus increases, $N_{\rm e}$ decreases, and the tube diameter drops. For sufficiently stiff chains, we pass out of the regime where LN applies.

The opposite limit of stiff chains in a dilute solution, with the persistence length much longer than the tube diameter, has been considered by Morse. His physical picture is that the entanglement length for stiff chains is the distance over which

transverse deflections under thermal fluctuations of a given chain segment are sufficient to intercept a second chain segment on an oblique path. In this regime, the tube diameter a, entanglement arclength $L_{\rm e}$ (physical length of an entanglement strand), and Kuhn length $L_{\rm K}$ satisfy the inequalities $a < L_{\rm e} < L_{\rm K}$. The Morse scaling ansatz predicts power law scaling for G as a function of concentration and chain stiffness, consistent with experimental data on entangled solutions of biological filaments such as F-actin.

A different approach to scaling predictions for both stiff and flexible chains was introduced by Everaers. ^{23–25} Rather than constructing a scaling theory that predicts specific power law dependence of G on the volume fraction ϕ , Kuhn length $L_{\rm K}$, and chain diameter d, Everaers asserted that the dependence of entanglement properties on ϕ and d should come only through the combination ϕ/d^2 , with $L_{\rm K}$ then the only independent microscopic length in the problem. This combination ϕ/d^2 is the arclength density, i.e., the total chain length per unit volume. The essence of Everaers' assertion is that the thickness of the chain does not matter for uncrossability, which intuitively makes sense if the chains are regarded as thin threads of some irrelevantly small diameter d.

Everaers' thread scaling ansatz implies that the plateau modulus G should scale as $kT/L_{\rm K}^{\ 3}$ times a dimensionless function of $(\phi/d^2)L_{\rm K}^{\ 2}.^{2.5}$ This assertion can be tested by plotting $\beta GL_{\rm K}^{\ 3}$ versus $(\phi/d^2)L_{\rm K}^{\ 2}$ for chains of different stiffness, diameter, and volume fraction; if the assertion holds, a master curve should result. Remarkably, a wide range of simulation data on entanglement properties of flexible and stiff bead-spring chains and solutions as well as experimental data on stiff chains do fall on such a master curve. The master curve exhibits a crossover, from a power law characteristic of the stiff chain regime at large values of $(\phi/d^2)L_{\rm K}^{\ 2}$ (i.e., stiff chains, not too dilute) to a second power law regime at small $(\phi/d^2)L_{\rm K}^{\ 2}$.

However, the thread scaling ansatz is not consistent with LN as generalized above to solutions, i.e., with G scaling as $kT/p^3\phi^2$, which describes a wide range of flexible polymer melts and solutions. To see this, observe that LN as generalized to solutions implies βGL_K^3 scales as $\phi^2(L_K/d)^6$. In contrast, starting with G scaling as kT/p^3 in the melt, the thread scaling ansatz implies G must scale as ϕ^3 , which is definitely ruled out by experiments on solutions. Alternatively, starting with G proportional to ϕ^2 , the thread scaling ansatz implies G scales as $kT\phi^2/(p^2L_K)$, which is not consistent with the observed LN scaling, $G \sim kT/p^3$ for flexible chain melts.

In short, the thread scaling ansatz is consistent with data on stiff chains, and crosses over to describe simulation results for more flexible bead-spring chains, but is not consistent with experimental data on real flexible melts and solutions. Because the thread scaling master curve already displays a crossover but does not include the LN regime, it suggests we have missed a scaling regime between LN for flexible chains and Morse for stiff chains. Indeed, we shall argue below that the missing scaling regime corresponds to thin flexible threadlike chains, for which the packing length p is smaller than d. If p is less than d, p becomes irrelevant to governing the typical distance of close approach between chain segments, and the LN regime cannot apply.

In the present work, we propose a consistent scaling description that encompasses the LN, flexible threadlike, and Morse stiff chain regimes, and describes two crossovers from

flexible chains all the way to stiff chains, as well as the volume fraction dependence of each regime. Moreover, we present a consistent physical picture of what constitutes an entanglement, which reconciles the LN description of "cohabiting" entangled strands as somehow giving rise to entanglements, with the Morse description of "intercepting" chain segments as directly resulting in binary entanglement interactions. We shall show that the Morse physical description can be extended to the flexible threadlike and LN regimes.

We shall describe in addition how solvent quality affects entanglement. For sufficiently dilute solutions and good solvents, individual chain segments exhibit self-avoidance within a correlation volume or "blob". This changes the probability that two chain segments will encounter each other and entangle. A crossover occurs at the swelling concentration ϕ_s between two distinct regimes of entanglement scaling: the Edwards regime of ideal random walk chains for ϕ above ϕ_s , and the semidilute regime of locally self-avoiding chains for ϕ below ϕ_s . In these two regimes, the modulus G depends on ϕ with different power laws. By enforcing continuity across this boundary, we extend our scaling theory and discover how likely binary contacts are to occur in the semidilute regime.

In short, we present in this paper a comprehensive scaling theory of entanglement in melts and solutions of flexible and stiff polymer chains. The paper is organized as follows. First, we summarize the assumptions and results of the Lin-Noolandi scaling theory for flexible chains, followed by the Morse scaling theory for stiff chains. Then, we present a regime plot as a function of chain stiffness and concentration, in which the boundaries of validity of the LN and Morse regimes are shown, and additional scaling regimes indicated, anticipating results of forthcoming sections. Next, we describe the semiflexible threadlike regime, and present estimates of the numerical values of scaling prefactors. Finally, we describe the crossover for entanglement in good solvents from the Edwards regime to semidilute solutions.

LIN-NOOLANDI SCALING

In the Lin-Noolandi regime of entangled flexible chains, entanglement strands are assumed flexible enough that they can be described by random walks within the tube:

$$a \gg L_{\rm K}$$
 (1)

The basic scaling assumptions of the Lin-Noolandi ansatz are as follows. $^{13-15}$

(1) The entanglement modulus G scales as kT per entanglement strand volume:

$$G \sim \frac{kT\phi}{N_{\rm e}\Omega_0} \sim \frac{kT\phi}{(N_{\rm e}/N_{\rm K})\Omega_{\rm K}}$$
 (2)

(We will find it convenient in what follows to measure chain length in Kuhn segments; here Ω_0 is the volume of a monomer, and Ω_K is the volume of a Kuhn segment.)

(2) The tube diameter *a* is the mean-square end-to-end distance of an entanglement strand:

$$a^2 \sim N_{\rm e}b^2 \sim \frac{N_{\rm e}}{N_{\rm K}}L_{\rm K}^2 \tag{3}$$

(3) The packing length is a material parameter, defined as the ratio of displaced volume to mean-square end-to-end distance, both of which scale linearly with chain length.

$$p \sim \frac{\Omega}{R^2} = \frac{\Omega_K}{L_K^2} \tag{4}$$

Roughly speaking, the packing length is the scale at which monomers near to a given monomer come predominately from nearby monomers along the chain. Thus, *p* governs the closest approach distance of monomers on two distinct chain segments (Figure 4).

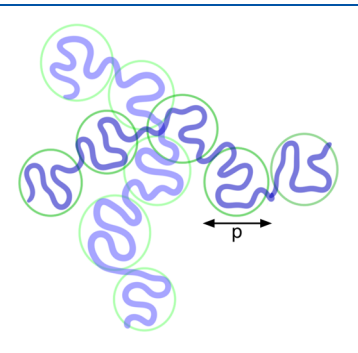


Figure 4. Cartoon of chain as random walk of "packing blobs", which govern typical close-approach distance between chain segments.

We envision the chain as a continuous path with Kuhn length $L_{\rm K}$ and diameter d. We expect that $L_{\rm K}/d$ must be larger than unity, since we cannot easily bend a chain on a radius tighter than its own space-filling diameter. With that limitation, we can imagine a family of chains of increasing stiffness, measured by the ratio $L_{\rm K}/d$.

For flexible bead-spring chains, the Kuhn length is about one step, i.e., $L_{\rm K}=d$. For bead-spring chains with explicit bending energy, represented by interactions between adjacent steps of the form $U(\theta)=(1/2)\kappa\theta^2$, the persistence length is $L_{\rm p}=\beta\kappa$ and Kuhn length is $L_{\rm K}=2L_{\rm p}$, with a smooth crossover to $L_{\rm K}=d$ at small $\beta\kappa$.

The Kuhn volume $\Omega_{\rm K}$ scales as $\Omega_{\rm K} \sim d^2 L_{\rm K}$. Correspondingly, the packing length can be written as $p = C d^2 / L_{\rm K}$, where C is a coefficient of order unity. Hence, we have $p/L_{\rm K} \sim (d/L_{\rm K})^2$. As usual in writing such scaling relations, we typically omit coefficients of order unity. Later, we shall use results from bead-spring simulations to estimate the coefficient C.

(4) The tube diameter is proportional to the packing length. This is a consequence of the Lin-Noolandi ansatz, that a fixed number of entanglement strands cohabit the pervaded volume of an entanglement strand, which implies that $R_e^3 \sim N_e \Omega_0$. Since R_e scales as a and $N_e \Omega_0 / R_e^2$ scales as p, we have

$$a \sim p$$
 (5)

(5) Entanglements are regarded as binary events, so that upon dilution we have

$$N_{\rm e}(\phi) = N_{\rm e}/\phi \tag{6}$$

where $N_{\rm e}$ is the entanglement length in the corresponding melt. As a consequence of these scaling assumptions, we can write

$$N_{\rm e}\Omega_0\sim p^3\phi^{-1}$$

$$G \sim \frac{kT}{p^3} \phi^2 \tag{7}$$

Below, we shall give alternative physical arguments that lead to the same scaling as Lin-Noolandi, but are more easily extended to semiflexible chains and solutions.

Note that the Kuhn length $L_{\rm K}$ appears nowhere in these scaling assumptions, except that implicitly $L_{\rm K} < a$ because the chain is assumed flexible within its tube.

It is useful to express the tube diameter, entanglement length, and modulus in comparison to some characteristic microscopic parameters. Because there are multiple microscopic lengths $(d, L_{\rm K}, p)$ in the problem, there are many ways to do this. One appealing way is to compare a to $L_{\rm K}$, $N_{\rm e}$ to $N_{\rm K}$, and G to $kT/\Omega_{\rm K}$. For a and $N_{\rm e}$, these comparisons directly assess whether the scaling is valid (since we need $a/L_{\rm K}>1$ and $N_{\rm e}/N_{\rm K}>1$ to use these results). We have

$$(a/L_{\rm K})^2 \sim (N_{\rm e}/N_{\rm K}) \sim (d/L_{\rm K})^4 \phi^{-1}$$

 $G \sim (kT/\Omega_{\rm K}) \phi^2 (L_{\rm K}/d)^4$ (8)

MORSE SCALING

The complementary limit of entangled semiflexible chains is described by Morse scaling, which assumes chains are stiff within the tube (Figure 5), that is

$$a \ll L_{K}$$
 (9)

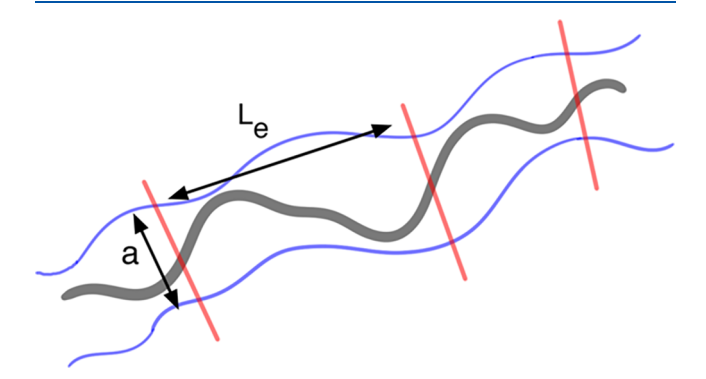


Figure 5. Cartoon of a stiff chain confined to its tube.

The scaling assumptions of the Morse ansatz are as follows. ^{21,22}

(1) The tube diameter a is given by transverse displacements of stiff entanglement strands of length $L_{\rm e}$, which bend slightly by thermal fluctuations, on a radius of order $L_{\rm K}$ (Figure 6):

$$a^2 \sim \frac{L_{\rm e}^3}{L_{\rm K}} \tag{10}$$

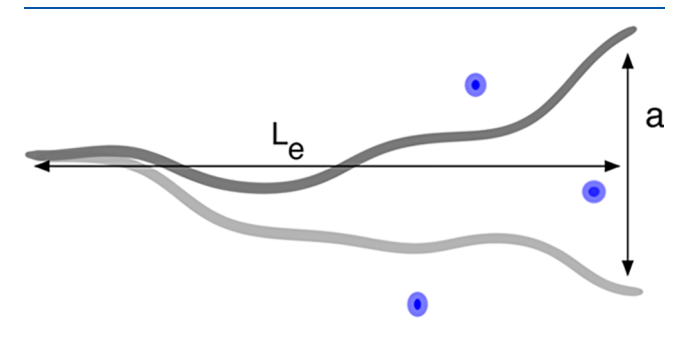


Figure 6. Cartoon of the area swept out by a fluctuating stiff chain segment, which may intercept a second obliquely oriented chain segment.

To see this, consider that the chain tangent makes a random walk on the unit sphere (starting at $\hat{n}=\hat{z}$, say). The transverse displacement t of the tangent vector over a short chain segment of length L scales as $t^2 \sim L/L_{\rm K}$. In turn, the magnitude t scales as Δ/L where Δ is the transverse displacement of the far end of the segment.

(2) Of order one "near miss" occurs between a given entanglement strand and some other such strand. (Note that this assumes entanglements are binary events.) We estimate the probability of such an interaction as the product of an "intercept area" of order aL_e , times the arclength density ρ (chain arc length per volume):

$$\rho a L_{\rm e} \sim 1 \tag{11}$$

(3) For a solution of semiflexible chains, the arclength density scales as

$$\rho \sim \frac{\phi L_{\rm K}}{\Omega_{\rm K}} \sim \frac{\phi}{d^2} \tag{12}$$

in which d is the monomer diameter and hence the diameter of the strand.

(4) The entanglement modulus is again kT per entanglement strand

$$G \sim \frac{kT\rho}{L_{\rm e}} \sim \frac{kT\phi}{(L_{\rm e}/L_{\rm K})\Omega_{\rm K}}$$
 (13)

Putting these assumptions together, we have the following results: the entanglement arclength scales as

$$\frac{L_{\rm e}}{L_{\rm K}} \sim \phi^{-2/5} (d/L_{\rm K})^{4/5}$$
 (14)

The tube diameter scales as

$$\frac{a}{L_{\rm K}} \sim \phi^{-3/5} (d/L_{\rm K})^{6/5} \tag{15}$$

Finally, the plateau modulus scales as

$$G \sim \frac{kT}{\Omega_{\rm K}} \phi^{7/5} (L_{\rm K}/d)^{4/5}$$
 (16)

Note that in this scaling argument, two independent microscopic lengths appear $(d \text{ and } L_{\rm K})$, instead of just one (p) as for flexible chains.

Because of the multiplicity of microscopic lengths, there are many equivalent ways of expressing these scaling laws. In some sense, it is natural to consider d and $L_{\rm K}$ as the two fundamental parameters describing the geometry of a semiflexible chain, which in the simplest representation has a persistence length and a diameter. (Therefore in the above, we have expressed stiffness in terms of the ratio $L_{\rm K}/d$, which we expect should be greater than unity.)

Implicit in the Morse scaling ansatz is that the chain diameter is irrelevant in counting "near misses" between stiff chain segments. For sufficiently concentrated stiff chains, this assumption may break down, as suggested by the results and arguments of Tassieri, ²⁶ who analyzed data from semiflexible solutions in what he called the "tightly entangled concentration regime".

Nematic Phase. For sufficiently stiff and concentrated chains, we expect to encounter a nematic phase, which preempts a portion of the semiflexible regime. For completely rigid rods, the Onsager prediction for the nematic phase boundary can be obtained from a simple scaling argument, as follows.

For isotropically oriented rods, the probability P that a given randomly placed rod will collide with some other rod in some other orientation scales as $P \sim L^2 dc$, where the rods have length L and diameter d, and the concentration of rods is c. (This follows from the fact that for an arbitrary oblique angle between the rods, the excluded region for placing a second rod center has volume of order $L^2 d$.) This concentration c is related to the volume fraction ϕ by $\phi \sim cLd^2$. The collision probability becomes entropically untenable when P becomes of order unity, so that the nematic transition is predicted to occur when $\phi \sim d/L$.

The Khokhlov–Semenov model essentially represents the semiflexible chain as a sequence of randomly oriented straight segments of length $L_{\rm K}$. Their prediction for the nematic phase boundary scales as

$$\phi_{\rm IN} \sim \frac{d}{L_{\rm K}}$$
 (17)

which is a line of slope -1 in the regime plot, extending from some point along the melt line ($\phi = 1$) downward and to the right (see Figure 7).

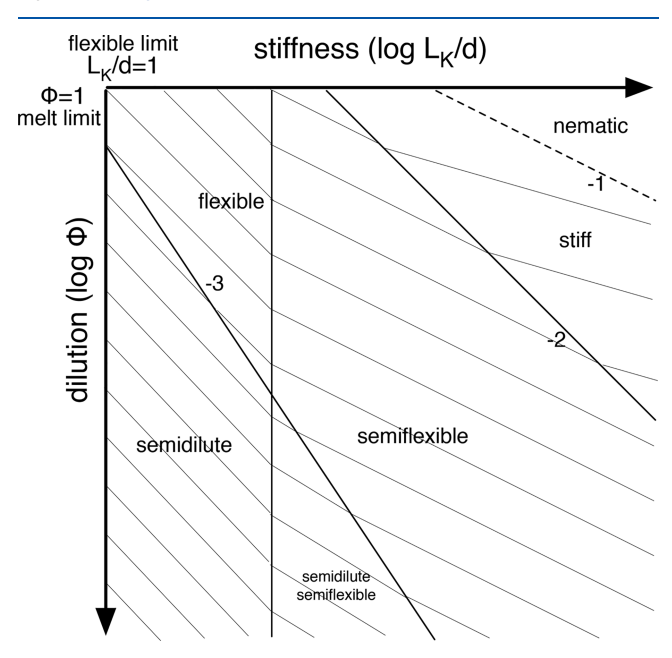


Figure 7. Regime plot of flexible (Lin-Noolandi), semidilute, semiflexible, and stiff (Morse) scaling regions with the Khokhlov–Semenov nematic phase boundary (dashed). Thin lines indicate constant $\beta\Omega_{\rm K}G$.

■ REGIME PLOT

Now we consider the limits of validity for the Morse and LN scaling. Morse assumes $a \ll L_{\rm K}$, so this scaling picture certainly cannot hold beyond $a \approx L_{\rm K}$, which from the scaling result for a, implies $\phi \geq (d/L_{\rm K})^2$. At this point, we likewise have $L_{\rm e}$ comparable to $L_{\rm K}$ (whereas within the semiflexible regime of validity, we have $a \ll L_{\rm e} \ll L_{\rm K}$). Therefore, for a dilute solution (with $\phi \ll 1$), for Morse scaling to be applicable, we must have chains sufficiently stiff and concentrated that $(d/L_{\rm K})^2$ is less than ϕ , so that a is then smaller than $L_{\rm K}$.

We can likewise inquire about the limit of validity of Lin-Noolandi scaling, which assumes flexible chains inside the tube, and thus $L_{\rm K}\ll a$. Reviewing the scaling relations eq 8 for the

flexible tube, the limit of validity of the Lin-Noolandi regime would appear to be $\phi \leq (d/L_{\rm K})^4$. That is, the system must be sufficiently dilute and flexible that ϕ is less than $(d/L_{\rm K})^4$. (Evidently, there is a coefficient of order unity in this inequality, which we have not written explicitly in any of our scaling relations.)

Note that this is a different power law relating the limiting stiffness and dilution than we found for the semiflexible regime. These two limiting boundaries do not coincide; the stiff regime boundary $\phi = (d/L_{\rm K})^2$ lies distinctly to the right of the boundary $\phi = (d/L_{\rm K})^4$ in the stiffness—dilution plane of values for $\log(L_{\rm K}/d)$ and ϕ . This is a hint that we have missed a scaling regime somewhere.

In fact, the Lin-Noolandi regime breaks down on increasing $L_{\rm K}/d$ even before the limit $\phi=(d/L_{\rm K})^4$ is reached. As the chains become more semiflexible, the packing length $p=Cd^2/L_{\rm K}$ decreases. Whatever the numerical coefficient C may be, eventually p will become as small as d. However, the packing length was meant to describe the distance of closest approach for two chain strands, limited by the tendency of flexible chain segments to fill nearby space with their own monomers. When chains are sufficiently rigid, p is irrelevant, and the distance of closest approach is set by d. Thus, the limit of the Lin-Noolandi regime is some finite value of $L_{\rm K}/d$, independent of concentration.

It is useful to represent the various scaling regimes in a "regime plot", log—log with the horizontal axis $L_{\rm K}/d$ and the vertical axis ϕ . The horizontal axis starts at $L_{\rm K}/d=1$ (the most flexible chain) and increases; the vertical axis starts at $\phi=1$ (the melt) and decreases. (See Figure 7.) The faint lines in the plot are lines of constant reduced modulus $\overline{G}=\beta G\Omega_{\rm K}$. In the flexible regime, the reduced modulus is constant on lines of slope -2, while in the stiff regime, lines of constant \overline{G} have slope -4/7.

Evidently, there is a previously unidentified regime between the "flexible" Lin-Noolandi regime and the "stiff" Morse regime, labeled "semiflexible" in the diagram. In the next section, we give scaling arguments to describe entanglement in the semiflexible regime.

One caveat about Figure 7: without knowing numerical prefactors for scaling results in the various regimes, we cannot know precisely where to draw the boundaries of the semifexible regime, but only what their slopes should be. We have placed the flexible—semiflexible and semiflexible—stiff boundaries to give a visible range of the semiflexible regime in the melt limit ($\phi = 1$). Independent of prefactors, the figure shows the semiflexible regime grows progressively wider in chain stiffness for more dilute solutions.

SEMIFLEXIBLE REGIME

One important difference between the flexible (Lin-Noolandi) and stiff (Morse) regimes is that in the stiff regime, the modulus does not "know" the chain diameter, but only how much chain arclength there is per unit volume. More precisely, G only depends on the volume fraction ϕ and chain diameter d through the combination ϕ/d^2 . This combination can be identified as the arclength density, i.e., the chain arclength per unit volume (as can be seen by writing it as ϕ times $L_{\rm K}/\Omega_{\rm K}$, where $\Omega_{\rm K} \sim d^2 L_{\rm K}$ is the volume of a Kuhn segment). In the stiff chain regime, the modulus can be written as

$$G \sim kT(\phi/d^2)^{7/5}L_K^{-1/5}$$
 (18)

which evidently depends on ϕ and d only through the arclength density ϕ/d^2 .

That is, the stiff chain regime is consistent with the "thread scaling" ansatz introduced by Everaers, who posited that entangled melts and solutions could be described only in terms of the arclength density. This ansatz implies that starting with one entangled melt or solution, we can reach another equivalently entangled system by shrinking d by some factor of λ , while holding $L_{\rm K}$ and the arclength density ϕ/d^2 fixed. (Thus, we shrink the volume fraction ϕ by a factor of λ^2 , which accounts for the reduced chain cross-sectional area at fixed arclength density.) Note that the ansatz does not by itself imply a particular power law dependence of G on ϕ . For any exponent α , $kT(\phi/d^2)^\alpha L_{\rm K}^{2\alpha-3}$ is a dimensionally consistent expression for G, depending only on ϕ/d^2 and $L_{\rm K}$.

In contrast, the flexible Lin-Noolandi regime is not consistent with the thread scaling ansatz. In this regime, G depends on ϕ and d separately, and cannot be written as a function only of ϕ/d^2 . Physically, we may say that the flexible regime "knows" about the packing length p, which governs the typical distance of closest approach between chain segments. In short, if we choose $\alpha=2$ to give G scaling as ϕ^2 , the resulting G does not scale as kT/p^3 in the melt. If instead we require that G scales as kT/p^3 in the melt, recalling that p scales as $d^2/L_{\rm K}$, we find $\alpha=3$, which implies G would scale as ϕ^3 . This result is not consistent with the observed scaling $G\sim \phi^2$ for real chains diluted by oligomeric marginal solvent.

However, one can envision a regime of semiflexible entangled threads, in which entanglements are still binary events (as in the Morse scaling ansatz for stiff chains), but now between semiflexible threads, for which the distance of closest approach is not p but simply d. In such a regime, the modulus would scale as

$$G \sim kT(\phi/d^2)^2 L_K \tag{19}$$

This form would be required by dimensional analysis, since we have asserted that ϕ and d should only enter in the combination ϕ/d^2 , and the only microscopic length remaining to give G the proper dimensions is L_K .

We can recast the scaling form of eq 19 as

$$G \sim \frac{kT}{\Omega_{\rm K}} \phi^2 \left(\frac{L_{\rm K}}{d}\right)^2 \tag{20}$$

Identifying G as kT per entanglement strand, the corresponding scaling form for N_e would be

$$\frac{N_{\rm e}}{N_{\rm K}} \sim \left(\frac{d}{L_{\rm K}}\right)^2 \phi^{-1} \tag{21}$$

Finally, the tube diameter in this regime would scale as

$$\frac{a}{L_{\rm K}} \sim \left(\frac{d}{L_{\rm K}}\right) \phi^{-1/2} \tag{22}$$

This putative scaling regime would end when $N_{\rm e}$ and $N_{\rm K}$ are the same order, that is, when $\phi \sim (d/L_{\rm K})^2$, which is the beginning of the stiff chain entanglement regime. This regime of entanglement between semiflexible threadlike chains would begin only when the packing length p was of order d, which is the end of the Lin-Noolandi flexible entanglement regime. Hence, this semiflexible entanglement regime sits between the Lin-Noolandi and Morse regimes, as required.

On the boundary between the stiff and semiflexible regimes, both regimes predict the modulus to scale as $G \sim kT/L_{\rm K}^3$, the entanglement weight $N_{\rm e}$ to scale as $N_{\rm K}$, and the tube diameter a to scale as $L_{\rm K}$. This is a very intuitive crossover between the stiff and semiflexible entangled regime: every Kuhn segment is marginally entangled.

On the boundary between the flexible and semiflexible regimes, p is of order d, which means $L_{\rm K}/d$ is some constant of order unity, whereupon both regimes predict the modulus to scale as $G \sim kT/\Omega_{\rm K}\phi^2$, the entanglement weight to scale as $N_{\rm e} \sim N_{\rm K}\phi^{-1}$, and the tube diameter as $a \sim L_{\rm K}\phi^{-1/2}$.

We can give a more physical picture of what is actually entangling in this semiflexible threadlike regime: Kuhn segments. A Kuhn segment randomly placed and thermally bent sweeps out an area of order $L_{\rm K}^2$ in the plane of its bend. If it intercepts another strand passing through this area, a binary entanglement may result. The area concentration of such strands scales as the thread arclength density ϕ/d^2 . Hence, the probability per Kuhn length P of such an encounter scales as $\phi(L_{\rm K}/d)^2$.

Over an entanglement weight $N_{\rm e}$, the probability of such an encounter is $PN_{\rm e}/N_{\rm K}$, which should be of order unity. Hence, we have

$$\frac{N_{\rm e}}{N_{\rm K}} \sim \left(\frac{d}{L_{\rm K}}\right)^2 \phi^{-1} \tag{23}$$

which is the threadlike scaling result. Combined with the assertion that the modulus G is kT per entanglement strand (which occupy a fraction ϕ of the volume), the semiflexible threadlike scaling for G follows.

The flexible Lin-Noolandi scaling regime can be described in the same way, except that the binary encounters are between packing blobs instead of Kuhn segments. The packing blobs have an effective diameter p (because two such strands can approach no closer) and an effective Kuhn length of p likewise (because a strand of packing blobs cannot bend more sharply than p). Thus, we expect to write

$$\frac{N_{\rm e}}{N_{\rm p}} \sim \phi^{-1} \tag{24}$$

in which $N_{\rm p}$ here denotes the number of monomers in a packing blob.

Since the packing blob is a Gaussian random walk, $N_{\rm p}$ scales according to

$$p^2 \sim \left(\frac{N_{\rm p}}{N_{\rm K}}\right) L_{\rm K}^2 \tag{25}$$

which together with $p \sim d^2/L_{\rm K}$ implies

$$\frac{N_{\rm p}}{N_{\rm K}} \sim \left(\frac{d}{L_{\rm K}}\right)^4 \tag{26}$$

Hence, this argument indeed implies the Lin-Noolandi scaling,

$$\frac{N_{\rm e}}{N_{\rm K}} \sim \left(\frac{d}{L_{\rm K}}\right)^4 \phi^{-1} \tag{27}$$

LN by Renormalization. A final argument for the Lin-Noolandi scaling regime is based on the idea that we can transform one melt into another with the same "topological

complexity", by a renormalization procedure of stiffening, shrinking, and fattening the chain at fixed p and fixed (melt) concentration (Figure 8). That is, we increase the Kuhn length

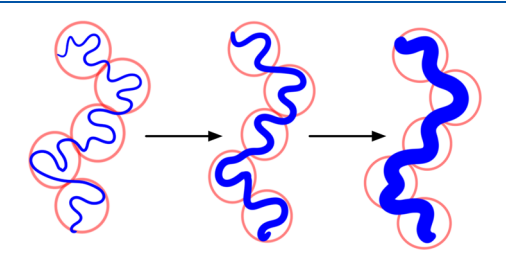


Figure 8. Cartoon of renormalization procedure by which one melt may be mapped onto another with fixed "topological complexity". The red circles correspond to packing blobs of size p.

by some factor λ , remove some arclength from along the chains to fix the mean-square end-to-end distance R^2 , and increase the monomer diameter to maintain constant p and melt concentration.

To implement this, we write $R^2 = LL_{\rm K}$, from which we see that to maintain fixed R^2 , the chain arclength L must decrease by a factor of λ . The chain displaced volume is Ld^2 , so to maintain melt conditions, d^2 must increase by a factor of λ . Hence, we have $L_{\rm K}' = \lambda L_{\rm K}$, $L' = L/\lambda$, and $d'^2 = \lambda d^2$, which implies that $p = d^2/L_{\rm K}$ remains constant under the renormalization.

Under this rescaling, d and L_K both grow, but L_K grows faster and started out larger than d in any case. Therefore, whatever the coefficient C in the scaling relation for p may be, L_K will become equal to p for some value of λ , which implies

$$\frac{L_{\rm K}^{\prime 2}}{d^{\prime 2}} \sim 1 \tag{28}$$

When this happens, we exit the Lin-Noolandi regime because the packing blob is no longer a flexible chain segment.

At the same time, the entanglement criterion begins to be met for each renormalized Kuhn segment: passing through the "interception area" of order $L'_{\rm K}^2$ of each renormalized Kuhn segment is some other strand (the renormalized arclength density being $1/d'^2$). Hence, each renormalized Kuhn segment is an entanglement strand in the renormalized melt. From the above relation, the value of λ for which this happens scales as

$$\lambda \sim \left(\frac{d}{L_{\rm K}}\right)^2$$
 (29)

Now, we work backwards, to find the number of original monomers that correspond to a renormalized Kuhn segment.

Suppose $L = L_e$ originally, then $L' = L'_K$. Using the renormalization relations above, we have $L_e = \lambda^2 L_K$, or

$$\frac{N_{\rm e}}{N_{\rm K}} \sim \left(\frac{d}{L_{\rm K}}\right)^4$$
 (30)

which is the Lin-Noolandi scaling for a melt, equivalent to $G \approx kT/p^3$.

■ ESTIMATE OF PREFACTORS

To this point, we have neglected numerical prefactors in all scaling relations, except for our assertion that the coefficient C in the relation $p = Cd^2/L_K$ must be significantly larger than unity (so that p is numerically larger than d for flexible chains).

Now we use results on the entanglement length for flexible bead-spring chains to estimate the coefficient C. From chain-shrinking methods, analysis of monomer mean-square displacement for entangled ring melts, and topological analysis, $N_{\rm e}$ for flexible bead-spring chains lies in the range of 60–70.

These flexible bead-spring chains have repulsive Lennard-Jones interactions,

$$U(r) = \epsilon (4((\sigma/r)^{12} - (\sigma/r)^6) + 1)$$
(31)

for $r<2^{1/6}\sigma$ and zero beyond. Bonded beads along the chain interact with a stiff harmonic potential, with a spring of rest length $2^{1/6}\sigma$. These chains are observed to be flexible enough that $N_{\rm K}=1$, i.e., $L_{\rm K}=2^{1/6}\sigma$, a single step along the chain. The bead concentration under "melt conditions", corresponding to $\phi=1$, has been taken as $c=0.7/\sigma^3$.

The effective hard-core diameter of the beads, at which the repulsive energy is 2kT, is $\sigma^* = 0.969\sigma$. We take σ^* as the effective diameter d of the chain. The corresponding effective volume per monomer is

$$\Omega_0 = (4\pi/3)(\sigma^*/2)^3 \tag{32}$$

To identify the prefactor in the scaling relation for p, we enforce $N_{\rm e}\Omega_0=p^3/\phi$ with $N_{\rm e}=65$, $\phi=1$, Ω_0 as above, and $d=\sigma^*$. This leads to p=3.24d. For this flexible bead-spring chain, from the above, we have $L_{\rm K}/d=1.16$ so that finally we have

$$p = 3.75d^2/L_{\rm K} \tag{33}$$

The flexible Lin-Noolandi regime ends when p=d, which implies that $L_{\rm K}=3.75d$. Since for chains with significant bending modulus we have the number of monomers per Kuhn length $N_{\rm K}$ equal to $2\beta\kappa$, the Lin-Noolandi regime ends when $\beta\kappa\approx 1.9$.

Intercept Probability. Another way to estimate numerical prefactors in our scaling relations is to bravely formulate a specific geometrical model for the probability per Kuhn length of an entanglement. This is most readily done in the threadlike semiflexible regime.

We model the strand that may hook around or "intercept" another oblique strand as a wormlike chain and approximate its trajectory as a circular arc with a radius governed by a Boltzmann factor of the bending energy. The intercepted area is taken to be bounded by the circular arc and its chord. We then determine the average number of strands that intersect this area, assuming these strands to be straight paths, randomly placed with isotropically distributed directions. We compute the average number of paths intercepted by averaging the intercept area over the bending angle of the circular arc, weighted by the Boltzmann factor. If the expected number of intercepted segments is well less than unity, we can interpret this number as the intercept probability.

The bending energy per segment in a discretized semiflexible chain is given by $(\kappa/2)\theta^2$, where κ is the bending stiffness of the angular spring. The tangent—tangent correlation function of this model can be computed in the limit of stiff springs as $\langle t_n \cdot t_0 \rangle = e^{-2na/L_{\rm K}}$. Here n is the number of segments in the path, the segment length is a, and $L_{\rm K}$ is the Kuhn length, given by $L_{\rm K} = 2\beta\kappa a$. The mean-square end-to-end distance of this semiflexible chain is $\langle R^2(n) \rangle = naL_{\rm K}$.

When a semiflexible path of length L is bent in a circular arc through an angle θ , we have $L = R\theta$, which allows us to convert back and forth between angle and radius. The total bending energy for such a circular arc is then $U = (\kappa/2)(a/R)^2 L/a$ (regarding the arc as L/a segments each bent by a small angle $\theta =$

a/R). We can write this in terms of the Kuhn length, replacing $K = kTL_K/(2a)$ as $U = (kT/4)L_K(1/R)^2L$.

From the geometry of the intercept area, we can write the intercept area as the difference between the area of a "wedge" cut from a disk and the area of two right triangles:

$$A = \frac{R^2 \theta}{2} - 2((1/2)(R \cos \theta/2))(R \sin \theta/2))$$
 (34)

Replacing R using $L=R\theta$ and using the double-angle formula, we obtain

$$A = \frac{L^2}{2} \left(\frac{1}{\theta} - \frac{\sin \theta}{\theta^2} \right) \tag{35}$$

For sufficiently stiff chains such that the deflection angle is small, we can expand $\sin\theta$ to obtain

$$A \approx \frac{L^2}{12}\theta\tag{36}$$

The Boltzmann factor governing the fluctuating area is

$$P(\theta) \propto e^{-(1/4)L_{\rm K}(1/R(\theta))^2L} = e^{-(1/4)(L_{\rm K}/L)\theta^2}$$
 (37)

From this, we can compute the average intercept area as

$$\langle A \rangle = \frac{L^2}{6\sqrt{\pi}} \left(\frac{L}{L_K}\right)^{1/2} \tag{38}$$

Now we compute the number of chain segments per unit area that cross the intercept area. We represent the other chain segments as straight paths of length L (the result will turn out to be independent of L). The concentration of these segments is

$$\rho = \frac{\phi}{\pi (d/2)^2} \tag{39}$$

which is the "arclength concentration" (chain arclength per unit volume) we introduced previously.

For a straight segment at an angle θ with respect to the intercept area normal, the segment will pass through the plane if the far end of the segment is within a distance $h = L\cos\theta$ of the plane. Therefore, the number of intersections per unit area is

$$N/A = \int \frac{d\Omega}{4\pi} \frac{\phi}{\pi (d/2)^2} L \cos \theta \tag{40}$$

in which the integral over solid angle averages over the orientation of the intercepted segments. Performing the integral, we obtain

$$N/A = \frac{2\phi}{\pi d^2} \tag{41}$$

The number of intercepted segments n_i for a fluctuating segment of length L_K is then

$$n_i = \frac{1}{3\pi^{3/2}} \left(\frac{L_{\rm K}}{d}\right)^2 \phi \tag{42}$$

If n_i is small compared to unity, we can interpret this number as the intercept probability per Kuhn segment. Its inverse is then the number of Kuhn segments per entanglement length,

$$\frac{N_{\rm e}}{N_{\rm K}} = 16.7 \left(\frac{d}{L_{\rm K}}\right)^2 \phi^{-1} \tag{43}$$

which scales like the threadlike semiflexible result, but now with an explicit value for the coefficient.

This result, combined with the numerical coefficient from the previous section, enables us to be more quantitative about the crossover from the Lin-Noolandi regime. The results $N_{\rm e}\Omega_0=p^3/\phi$ with $p=3.75d^2/L_{\rm K}$ and $\Omega_0=(4\pi/3)(d/2)^3$ can be written as

$$\frac{N_e}{N_{\rm K}} = 27.6 \left(\frac{d}{L_{\rm K}}\right)^4 \phi^{-1} \tag{44}$$

The crossover between the two regimes would then occur at $L_{\rm K}/d=1.28$, somewhat earlier than the previous estimate based on p=d. Evidently, simulation results in the threadlike semiflexible regime would be preferable to establish the value of the prefactor above and hence the crossover.

■ GOOD SOLVENT REGIME

Implicit in all the above scaling arguments is that the chain trajectories are uncorrelated, ideal random walks as they are in a melt or sufficiently concentrated solution. However, long chains in a good solvent at sufficiently low concentrations are described by the scaling theory of semidilute solutions. A semidilute solution consists of a dense packing of "correlation blobs" of size ξ , each of which consists of a portion of a single chain, with a self-avoiding random walk configuration. The trajectory of an entire chain in the semidilute solution is an ideal random walk of blobs (Figure 9).

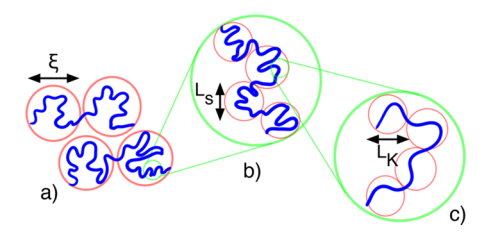


Figure 9. Cartoon of a chain in semidilute solution as a Gaussian random walk of correlation blobs, each of which is a self-avoiding walk of swelling blobs, each of which are Gaussian random walks of Kuhn segments.

The swelling of a single chain segment in good solvent begins to matter when the self-interaction energy of an unswollen, ideal random coil configuration becomes of order kT. This defines the swelling length N_s . An ideal random walk of N_s segments is a "thermal blob", of size L_s . As a semidilute solution becomes more concentrated, the correlation blob size ξ decreases. When ξ reaches L_s , a chain segment short enough to be isolated from neighboring segments is not long enough to swell. (Informally speaking, why should a chain in concentrated solution avoid itself, when it will run into other chains anyway?)

The above description can be cast as a set of scaling relations, as follows. The correlation length ξ is a self-avoiding walk of thermal blobs:

$$\xi \sim \left(\frac{g}{N_{\rm s}}\right)^{\nu} L_{\rm s} \tag{45}$$

in which *g* is the number of monomers in a blob, and $\nu = 0.588 \approx 3/5$ is the scaling exponent for self-avoiding walks.

The solution volume fraction ϕ is given by

$$\phi \sim \frac{g\Omega_0}{\xi^3} \tag{46}$$

Inside the thermal blob, the chain is an ideal random walk of Kuhn steps

$$\left(\frac{L_{\rm s}}{L_{\rm K}}\right)^2 \sim \frac{N_{\rm s}}{N_{\rm K}} \tag{47}$$

The condition for the swelling length is

$$\frac{(N_{\rm s}/N_{\rm K})^2 w_{\rm K}}{L_{\rm s}^3} \sim 1 \tag{48}$$

Here w_K is the excluded volume per Kuhn segment. The excluded volume characterizes the solvent quality, and hence the strength of self-avoidance. For a good solvent, w_K takes on a value characteristic of monomers that do not overlap. As a solvent becomes marginal, attractions between monomers decrease w_K . For semiflexible chains in good solvents, the expected value of w_K is of order dL_K^2 , which is the excluded volume for a pair of Kuhn segments at a random oblique angle. Therefore, we may write w_K as

$$w_{\rm K} \sim f dL_{\rm K}^{2} \tag{49}$$

in which the factor f<1 characterizes the solvent quality (f \rightarrow 0 is a marginal solvent).

We can solve the pair of scaling relations involving ξ and g to obtain

$$\frac{\xi}{L_{\rm s}} \sim \left(\frac{\phi L_{\rm s}^3}{\Omega_{\rm s}}\right)^{\nu/(1-3\nu)\approx -3/4} \tag{50}$$

The swelling criterion can be rewritten as

$$\frac{L_{\rm s}}{L_{\rm K}} \sim \frac{L_{\rm K}}{d} f^{-1} \tag{51}$$

(The swelling length is always larger than the Kuhn length, because $L_{\rm K}$ is greater than d and f is less than unity.) With this result, we can rewrite the ratio $L_{\rm s}^{\ 3}/\Omega_{\rm s}$ as

$$\frac{L_{\rm s}^3}{\Omega_{\rm s}} = \frac{L_{\rm K}^2}{\Omega_{\rm K}} L_{\rm s} \sim \left(\frac{L_{\rm K}}{d}\right)^3 f^{-1} \tag{52}$$

Using these results in the expression above for ξ/L_s , we obtain

$$\frac{\xi}{L_{\rm K}} \sim \phi^{-3/4} \left(\frac{d}{L_{\rm K}}\right)^{5/4} f^{-1/4}$$
 (53)

The crossover to the marginal solvent regime in which chain trajectories are uncorrelated random walks happens when ξ is comparable to $L_{\rm s}$. From the above expression for $\xi/L_{\rm s}$, this occurs when the volume fraction satisfies

$$\phi = \phi_{\rm m} \sim f \left(\frac{d}{L_{\rm K}}\right)^3 \tag{54}$$

It is often said that in semidilute solutions there is only one length scale, namely the correlation length ξ . One might then naively suppose that the entanglement modulus for a semidilute solution should scale as kT per blob,

$$G \sim \frac{kT}{\xi^3} \tag{55}$$

in that the tube diameter a should scale as ξ itself, and the entanglement arclength $N_{\rm e}$ as $g.^{31}$

However, this is clearly inconsistent with the scaling result in the flexible Lin-Noolandi regime on the marginal solvent boundary. To see this, note that kT per blob on this boundary would imply

$$G \sim \frac{kT}{\Omega_{\rm K}} \left(\frac{d}{L_{\rm K}}\right)^{\rm S} f^{3} \tag{56}$$

which is not consistent with the flexible regime on this boundary,

$$G \sim \frac{kT}{\Omega_{\rm K}} \left(\frac{d}{L_{\rm K}}\right)^2 f^2 \tag{57}$$

The inconsistency arises from the fact that there is not just of order one entanglement per correlation blob. Correlation blobs do not interact like impenetrable hard spheres; indeed, the free energy cost to overlay two blobs is only of order kT. What correlation blobs do is reduce the likelihood of contact between chain segments. To quantify this effect, we argue as follows.

The interaction free energy per unit volume F_s in the semidilute regime really does scale as kT per blob; with the above scaling relations, this leads to

$$F_{\rm s} \sim (kT/\Omega_{\rm K})\phi^{9/4} (L_{\rm K}/d)^{7/4} f^{3/4}$$
 (58)

In the marginal solvent regime where chain segments are uncorrelated, the interaction free energy per unit volume $F_{\rm m}$ scales as the sum of random pairwise interactions between Kuhn segments,

$$F_{\rm m} \sim kTw_{\rm K}(\phi/\Omega_{\rm K})^2 \sim (kT/\Omega_{\rm K})\phi^2(L_{\rm K}/d)f$$
 (59)

On the marginal solvent boundary, $F_{\rm s}$ equals $F_{\rm m}$. Below the boundary, in the semidilute regime, $F_{\rm s}$ is smaller than $F_{\rm m}$ by a factor of

$$\frac{F_{\rm s}}{F_{\rm m}} \sim \phi^{1/4} (L_{\rm K}/d)^{3/4} f^{-1/4} \tag{60}$$

This factor may be interpreted as the decreased likelihood of binary contacts relative to random mixing.

We assert that the number of binary contacts between packing blobs in semidilute solution should be estimated with the same decreased likelihood, relative to the flexible chain regime in which marginal solvent conditions prevail. Thus, the semidilute entanglement arclength $N_{\rm e}$ should increase relative to the flexible regime by a factor of $F_{\rm m}/F_{\rm s}$:

$$\frac{N_{\rm e}}{N_{\rm K}} \sim \phi^{-5/4} (d/L_{\rm K})^{19/4} f^{1/4} \tag{61}$$

The entanglement modulus is then once again kT per entanglement strand,

$$G \sim \frac{kT\phi}{N_{\rm e}\Omega_0} \sim (kT/\Omega_{\rm K})\phi^{9/4} (L_{\rm K}/d)^{19/4} f^{-1/4}$$
 (62)

By construction, this scaling form for G in the semidilute region agrees with the Lin-Noolandi scaling form along the marginal solvent boundary. It also scales with volume fraction as $\phi^{9/4}$, the same way as the interaction free energy per volume F_s . However, it is not the same as F_s ; the ratio is

$$\frac{G}{F_{\rm s}} \sim (L_{\rm K}/d)f^{-1} = 1/\phi_{\rm m}$$
 (63)

which is evidently larger than unity. This reflects the fact that there are many entanglement points per correlation blob, not just one.

In this regime, lines of constant $eta\Omega_{
m K}G$ satisfy the scaling relation

$$\phi \sim \left(\frac{L_{\rm K}}{d}\right)^{-19/9} \tag{64}$$

which in the regime plot are lines of slope -19/9 (nearly equal to 2).

Finally, there must be also a "semidilute semiflexible" regime at very low concentrations of semiflexible chains, in which chains are threadlike and the packing length is irrelevant, but chains are still swollen by a good solvent. (See Figure 1.) The boundary of the semidilute regime extends beyond the vertical boundary separating the flexible and semiflexible regimes. Along this boundary, the "semidilute semiflexible" and "marginal solvent semiflexible" regimes must be continuous. At the vertical boundary, the "semidilute flexible" and "semidilute semiflexible" regimes must be continuous.

By enforcing continuity at the vertical boundary, we must have the entanglement modulus in this region scaling as $\phi^{9/4}$. Assuming this and enforcing continuity at the semidilute-marginal boundary, we obtain

$$G \sim (kT/\Omega_{\rm K})\phi^{9/4} (L_{\rm K}/d)^{11/4} f^{-1/4}$$
 (65)

This form is also consistent with the semidilute scaling form for G on the vertical boundary between the flexible and semiflexible regimes, along which $L_{\rm K}/d$ is some constant of order unity.

The corresponding scaling for the entanglement arclength is

$$\frac{N_{\rm e}}{N_{\rm K}} \sim \phi^{-5/4} (d/L_{\rm K})^{11/4} f^{1/4} \tag{66}$$

Lines of constant $\beta\Omega_{\rm K}G$ in this regime satisfy

$$\phi \sim (L_{\rm K}/d)^{-11/9} \tag{67}$$

CONCLUSIONS

In this paper, we have presented a comprehensive scaling theory of entanglement for melts and solutions of flexible, semiflexible, and stiff chains. We propose that there are five distinct scaling regimes for entanglement, distinguished by the answers to three questions: (a) are chains flexible in their tubes; (b) are chains flexible and bulky enough that the packing length p is larger than the chain diameter d; and (c) are solutions dilute enough that the swelling length L_s is smaller than the correlation length ξ ?

Our approach reconciles three prior theoretical efforts, which describe entanglement of (1) melts and concentrated solutions of chains sufficiently flexible and bulky that the packing length is relevant (Lin-Noolandi); 12–15 (2) melts and concentrated solutions of chains that are flexible but threadlike, such that the packing length is irrelevant (Everaers); 25 and (3) solutions of stiff chains, such that the Kuhn length is larger than the tube diameter (Morse). 21,22

The Lin-Noolandi ansatz for entanglement of flexible chains as originally formulated focuses on the number of chain segments cohabiting the pervaded volume of an entanglement. This appears quite different from the Morse approach to entanglement for stiff chains, which identifies an entanglement

as a binary event in which a transversely fluctuating chain segment intercepts a second, obliquely oriented segment. We reconcile these apparently disparate approaches by recasting the LN scaling argument in terms of the probability that two chain segments, each consisting of a sequence of "packing blobs", will intercept each other. Thus, in our formulation, the LN regime and its scaling are consistent with a picture of entanglements as binary events.

Throughout our scaling approach, in all five regimes, the entanglement length can be defined in terms of intercept probabilities between two strands; the regimes differ in the details of the strands. When the packing length is relevant (when p>d), the entangling strands are sequences of packing blobs; when the chain is threadlike and flexible in its tube, the entangling strands are Kuhn segments.

In solutions, the concentration dependence of the entanglement length and plateau modulus arise from estimating the probability that two entangling strands come close together. The entangling strands may be either sequences of packing blobs or Kuhn segments, depending on whether the packing length is larger than the chain diameter and thus relevant to typical close approaches between chains. In "mean-field" solutions of flexible chains, where the solvent is marginal enough and the concentration high enough that the correlation length is less than the swelling length, chains are Gaussian random walks on all scales above the Kuhn length. (This is the situation for dilution of polymer melts by unentangled oligomers, for example.) In this case, intercept probabilities for a given strand are reduced by a factor ϕ relative to the melt, by a simple deletion of a fraction $1 - \phi$ of material with no change in chain configurations. The plateau modulus G then scales as ϕ^2 , consistent with careful experiments. For semidilute solutions, the scaling result for G is a slightly stronger dependence on ϕ , because self-avoidance within the correlation blobs tends to keep chains apart, and so reduces the chance for an entanglement to form.

One important limitation of the present approach is that we only describe asymptotic scaling in each regime, as if that regime were far removed from others to which it crosses over. In other words, we predict scaling of G and $N_{\rm e}$ in the flexible (Lin-Noolandi) regime assuming that p is much larger than d and hence governs close approaches between chain segments. In practice of course, p and d are both microscopic lengths, and the semiflexible regime is never terribly far away. There will be crossover effects between these two regimes (and likewise, at the boundaries between mean-field and semidilute flexible solutions, and between semiflexible and stiff chain solutions). If we are lucky, the crossovers will be localized, and reasonable power-law behaviors will be observed in each regime, with exponents close to the asymptotic predictions.

We have emphasized that threadlike scaling as proposed by Everaers is not compatible with the scaling found by Fetters for a wide range of real polymers (G proportional to p^{-3}), combined with the observed concentration dependence for entangled polymers diluted with oligomers (G proportional to ϕ^2). However, threadlike scaling seems to be satisfied by all published simulation results on linear bead-spring chain melts and solutions, including chains with and without explicit angular springs.

Taken together, these two observations invite the question: where is polyethylene (PE), the "most entangled" polymer with the smallest value of p/d among the Fetters compilation of entanglement data for real polymers with single-bond back-

bones, with respect to the crossover to the threadlike semiflexible scaling regime? Likewise, where is the most flexible linear bead-spring chain with respect to the crossover to the flexible Lin-Noolandi scaling regime?

In principle, we would like to plot data for real polymer melts and bead-spring simulations together, as $\beta G L_{\rm K}^{\ 3}$ versus $L_{\rm K}/d$ (dimensionless modulus versus dimensionless measure of stiffness). However, for a fair comparison it is crucial to use the same definitions for real and simulated polymers of G, L_K , and d; otherwise, factors of order unity will creep in and spoil the comparison. If the present scaling theory is valid, real polymers should fall on one side of the LN-threadlike crossover and linear bead-spring polymers on the other. It should be possible to identify polymers slightly stiffer than PE but equally skinny, which would enter the threadlike regime, for which Lin-Noolandi scaling would fail. Correspondingly, we can design and simulate bead-spring polymers with larger values of p/d, which should show the expected but as-yet unseen Lin-Noolandi scaling; indeed, results of such simulations will be reported in a forthcoming paper.

AUTHOR INFORMATION

Corresponding Author

Scott T. Milner – Department of Chemical Engineering, The Pennsylvania State University, University Park, Pennsylvania 16802, United States; orcid.org/0000-0002-9774-3307; Email: stm9@psu.edu

Complete contact information is available at: https://pubs.acs.org/10.1021/acs.macromol.9b02684

Notes

The author declares no competing financial interest.

■ ACKNOWLEDGMENTS

The author thanks Ralph Colby, Enrique Gomez, Daniel Read, and Jian Qin for helpful conversations and NSF for support under DMR-1507980 and DMR-1629006.

REFERENCES

- (1) Doi, M.; Edwards, S. F. The Theory of Polymer Dynamics; Clarendon Press: Oxford, 1986.
- (2) Graham, R. S.; Likhtman, A. E.; McLeish, T. C. B.; Milner, S. T. Microscopic theory of linear, entangled polymer chains under rapid deformation including chain stretch and convective constraint release. *J. Rheol.* **2003**, *47*, 1171–1200.
- (3) Likhtman, A. E.; McLeish, T. C. B. Quantitative theory for linear dynamics of linear entangled polymers. *Macromolecules* **2002**, 35, 6332–6343.
- (4) McLeish, T. C. B.; Milner, S. T. Entangled dynamics and melt flow of branched polymers. *Adv. Polym. Sci.* **1999**, *143*, 195–256.
- (5) van Ruymbeke, E.; Bailly, C.; Keunings, R.; Vlassopoulos, D. A General Methodology to Predict the Linear Rheology of Branched Polymers. *Macromolecules* **2006**, *39*, 6248–6259.
- (6) Shchetnikava, V.; Slot, J. J. M.; van Ruymbeke, E. A Comparison of Tube Model Predictions of the Linear Viscoelastic Behavior of Symmetric Star Polymer Melts. *Macromolecules* **2014**, *47*, 3350–3361.
- (7) van Ruymbeke, E.; Nielsen, J.; Hassager, O. Linear and nonlinear viscoelastic properties of bidisperse linear polymers: Mixing law and tube pressure effect. *J. Rheol.* **2010**, *54*, 1155–1172.
- (8) Edwards, S. F. The statistical mechanics of polymerized material. *Proc. Phys. Soc.* **1967**, *92*, 9–16.
- (9) Edwards, S. F. The theory of rubber elasticity. Br. Polym. J. 1977, 9, 140–143.

- (10) Edwards, S. F. The theory of polymer solutions at intermediate concentration. *Proc. Phys. Soc.* **1966**, *88*, 265–280.
- (11) Graessley, W. W.; Hayward, R. C.; Grest, G. S. Excluded-volume effects in polymer solutions. 2. Comparison of experimental results with numerical simulation data. *Macromolecules* **1999**, *32*, 3510–3517.
- (12) Milner, S. T.; Lacasse, M.-D.; Graessley, W. W. Why χ Is Seldom Zero for Polymer Solvent Mixtures. *Macromolecules* **2009**, 42, 876–886.
- (13) Kavassalis, T. A.; Noolandi, J. New view of entanglements in dense polymer systems. *Phys. Rev. Lett.* **1987**, *59*, 2674–2677.
- (14) Kavassalis, T. A.; Noolandi, J. A New Theory of Entanglements and Dynamics in Dense Polymer Systems. *Macromolecules* **1988**, *21*, 2869–2879.
- (15) Lin, Y. H. Number of entanglement strands per cubed tube diameter, a fundamental aspect of topological universality in polymer viscoelasticity. *Macromolecules* **1987**, *20*, 3080–3083.
- (16) Fetters, L. J.; Lohse, D. J.; Richter, D.; Witten, T. A.; Zirkel, A. Connection between Polymer Molecular Weight, Density, Chain Dimensions, and Melt Viscoelastic Properties. *Macromolecules* **1994**, 27, 4639–4647.
- (17) Fetters, L. J.; Lohse, D. J.; Graessley, W. W. Chain dimensions and entanglement spacings in dense macromolecular systems. *J. Polym. Sci., Part B: Polym. Phys.* **1999**, *37*, 1023–1033.
- (18) Auhl, D.; Chambon, P.; McLeish, T. C. B.; Read, D. J. Elongational Flow of Blends of Long and Short Polymers: Effective Stretch Relaxation Time. *Phys. Rev. Lett.* **2009**, *103*, 136001–136004.
- (19) Shahid, T.; Huang, Q.; Oosterlinck, F.; Clasen, C.; van Ruymbeke, E. Dynamic dilution exponent in monodisperse entangled polymer solutions. *Soft Matter* **2017**, *13*, 269–282.
- (20) Milner, S. T. Predicting the tube diameter in melts and solutions. *Macromolecules* **2005**, *38*, 4929–4939.
- (21) Morse, D. C. Viscoelasticity of tightly entangled solutions of semiflexible polymers. *Phys. Rev. E* **1998**, *58*, R1237–R1240.
- (22) Morse, D. C. Tube diameter in tightly entangled solutions of semiflexible polymers. *Phys. Rev. E* **2001**, *63*, No. 031502.
- (23) Everaers, R.; Sukumaran, S. K.; Grest, G. S.; Svaneborg, C.; Sivasubramanian, A.; Kremer, K. Rheology and Microscopic Topology of Entangled Polymeric Liquids. *Science* **2004**, *303*, 823–826.
- (24) Sukumaran, S. K.; Grest, G. S.; Kremer, K.; Everaers, R. Identifying the primitive path mesh in entangled polymer liquids. *J. Polym. Sci., Part B: Polym. Phys.* **2005**, 43, 917–933.
- (25) Uchida, N.; Grest, G. S.; Everaers, R. Viscoelasticity and primitive path analysis of entangled polymer liquids: From F-actin to polyethylene. *J. Chem. Phys.* **2008**, *128*, No. 044902.
- (26) Tassieri, M. Dynamics of Semiflexible Polymer Solutions in the Tightly Entangled Concentration Regime. *Macromolecules* **2017**, *50*, 5611–5618.
- (27) Khokhlov, A. R.; Semenov, A. N. Liquid-Crystalline Ordering in the Solution of Long Persistent Chains. *Phys. A* **1981**, *108*, 546–556.
- (28) Khokhlov, A. R.; Semenov, A. N. Liquid-crystalline ordering in the solution of partially flexible macromolecules. *Phys. A* **1982**, *112*, 605–614.
- (29) Khokhlov, A. R.; Semenov, A. N. Liquid-crystalline ordering in solutions of semiflexible macromolecules with rotational-isomeric flexibility. *Macromolecules* **1984**, *17*, 2678–2685.
- (30) Khokhlov, A. R.; Semenov, A. N. On the theory of liquid-crystalline ordering of polymer chains with limited flexibility. *J. Stat. Phys.* **1985**, *38*, 161–182.
- (31) de Gennes, P.-G.; Scaling concepts in polymer physics; Cornell Univ. Press: Ithaca, New York, 1979.
- (32) de Gennes, P. G. Dynamics of Entangled Polymer Solutions. I. The Rouse Model. *Macromolecules* **1976**, *9*, 587–593.
- (33) de Gennes, P. G. Dynamics of Entangled Polymer Solutions. II. Inclusion of Hydrodynamic Interactions. *Macromolecules* **1976**, *9*, 594–598.